ConnectomeAtlas: Standalone 3D Multi-Scale Brain Connectome, Persistent Homology, and Lesion Workstation in Rust

Author: Bryan P. White (ORCID: 0000-0003-4191-3511) • **Affiliation:** CRV Science Labs • **Preprint ID:** APP-PREPRINT-21 (v0.8.0 Software Preprint) • **Categories:** q-bio.NC • cs.SI • cs.GR
Canonical DOI: 10.5281/zenodo.24359109 • **Apps Hub:** https://crvscience.com/apps • **Repository:** https://github.com/bpwhite/crvscience-connectome-atlas

Abstract — ConnectomeAtlas (v0.8.0) is an open-source, multi-scale 3D brain connectome and neuroinformatics workstation written in Rust across a five-crate workspace under GPL-3.0-or-later licensing. Unifying four curated anatomical presets spanning three orders of nervous-system complexity—Human MNI152 Macro-Connectome (40 regions, 62 tract systems), Mouse Allen CCFv3 (28 regions, 39 pathways), Drosophila melanogaster FlyWire (22 neuropils, 32 projections), and Caenorhabditis elegans WormAtlas (26 ganglion/nerve-cord nodes, 35 pathways)—the workstation pairs species-authentic procedural 3D anatomy meshes (gyral cortical hemispheres with surgical octant cutaway, foliated cerebellum, brainstem, corpus callosum, rodent olfactory bulbs, insect optic lobes and central complex, and C. elegans cuticle, two-bulb pharynx, and nerve ring) and synchronized 2D triplanar slice contours with weighted graph efficiency, clustering, rich-club coefficient, communicability, Kinouchi-Copelli excitable criticality (branching ratio sigma and dynamic range Delta), Jacobi symmetric control harmonics, and exact Z2 first-Betti (beta1) persistent homology within a deterministic CLI and interactive wgpu/egui 3D viewer. Verified across 12 workspace tests and binary CLI sweeps, all four species operate near criticality (sigma = 1.000, dynamic range 21.923–23.857 dB), with FlyWire attaining the strongest rich-club backbone (0.38095) and highest dynamic range (23.857 dB), C. elegans exhibiting peak clustering (0.28883), and Human MNI152 hosting 14 persistent beta1 topological cavities (max persistence 0.85). Simulated Human MNI152 lesions quantify cascading efficiency loss: severing the Cingulum Bundle lowers global efficiency to 80.34% (0.26475 to 0.21269, fragmenting into 2 components), severing the Corpus Callosum retains 87.82%, and ablating Posterior Cingulate hub DMN.PCC retains 88.31%, complemented by native NIfTI-1, TrackVis, SQLite WAL, SWC, and SHA-256 signed envelope I/O.

1. Introduction

Comparative connectomics increasingly demonstrates that conserved topological trade-offs—balancing short global routing paths against metabolic wiring cost, modular segregation, and rich-club backbone hubs—recur from nematode ganglia to human association cortex[1,2,5]. Yet software ecosystems for inspecting brain wiring remain heavily fragmented: tractography viewers rarely compute Z_2 algebraic homology cavities[4] or excitable dynamic range around branching criticality[3], whereas network-analysis scripts strip out 3D stereotaxic coordinates, white-matter bundles, and interactive virtual lesions.

ConnectomeAtlas (v0.8.0) consolidates comparative stereotaxic 3D streamline visualization, complex network graph theory, excitable branching criticality, exact 1D persistent homology, structural lesion testing, and neuroimaging file exchange inside a single dependency-free compiled Rust workspace (five workspace crates, `#![forbid(unsafe_code)]` in core analytics) within the CRV Science Open-Source Apps collection[6–25].

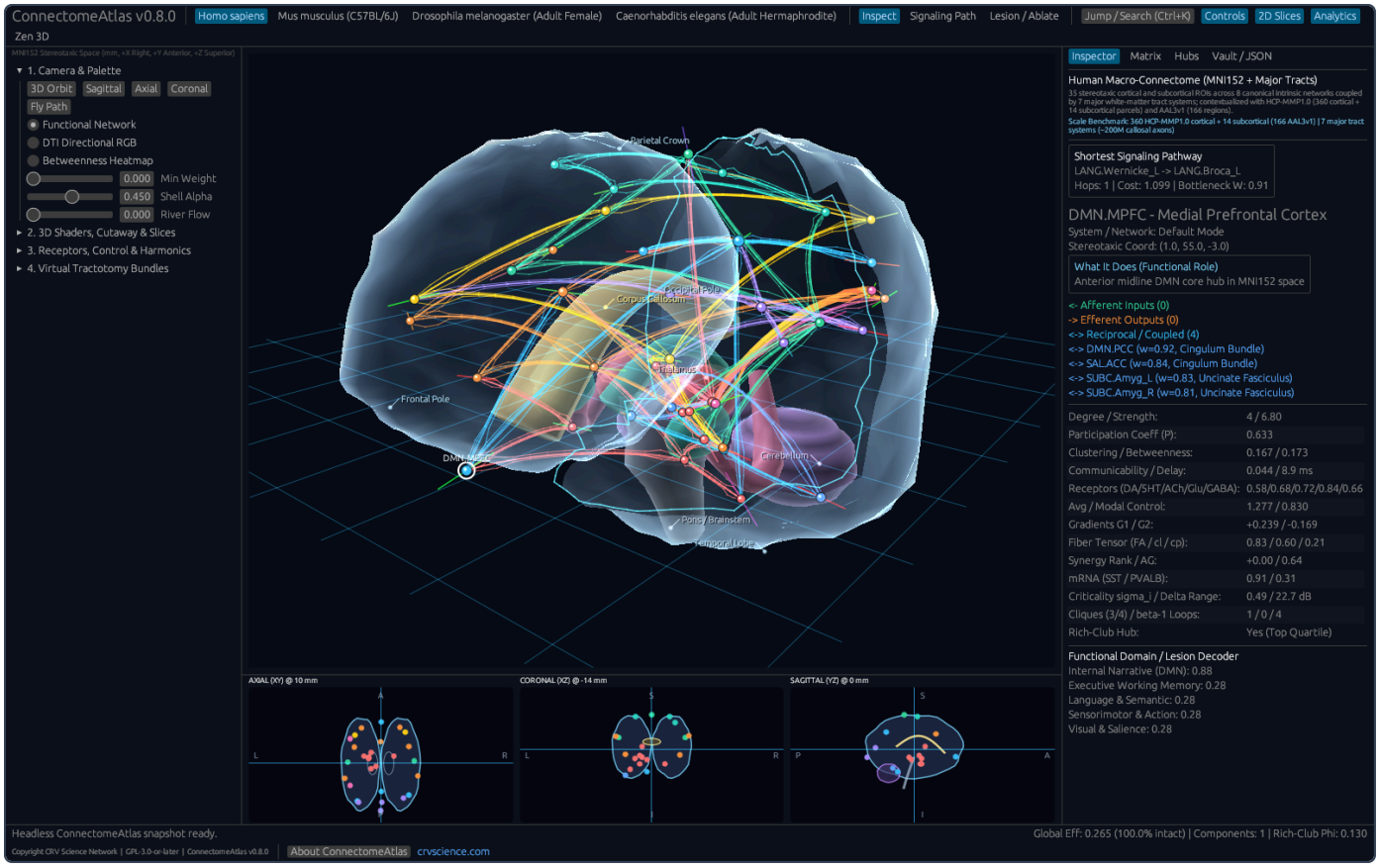
2. Multi-Scale Architecture & Topological Methods

ConnectomeAtlas is engineered as a modular five-crate Cargo workspace (Table 1). At initialization, each preset embeds nodes in authentic domain coordinates—millimeter MNI152 stereotaxic space for *Homo sapiens*, Allen CCFv3 coordinates for *Mus musculus*, scaled micrometer FAFB FlyWire neuropil centers for *Drosophila melanogaster*[5], and anterior-to-posterior body-axis positions for *Caenorhabditis elegans*. Alongside classical weighted efficiency, betweenness centrality, communicability, and rich-club stratification[2], `atlas-core` executes symmetric Jacobi eigendecomposition for network control harmonics, sweeps Kinouchi-Copelli excitable branching coupling around sigma = 1.0 to evaluate dynamic range (dB)[3], and builds descending weight-filtered clique complexes (`clique_3` , `clique_4`) with exact Z_2 boundary reduction to isolate persistent beta_1 loops[4].

Table 1. Five-Crate Workspace Architecture in crvscience-connectome-atlas v0.8.0

Workspace Crate / Files	Analytical & Systems Responsibilities
`crates/atlas-core` (9 files)	Connectome graph model, 4 species presets, shortest-path latency & lesion delta engine, Jacobi control harmonics, Kinouchi-Copelli criticality, exact Z_2 beta_1 TDA, systems transcriptomics, and command palette index.
`crates/atlas-io` (4 files)	Pure-Rust NIfTI-1 (`.nii` / `.nii.gz`) reader, TrackVis (`.trk`) streamline reader, SQLite WAL state vault, SHA-256 `AtlasEnvelope` JSON, and 3D `.swc` arbor exporter.
`crates/atlas-render` (5 files)	Species-authentic 3D anatomical surface/organ meshes & 2D MRI slice contours (`anatomy.rs`), custom arcball camera, braided streamline bundles, DTI tensors, and wgpu shader descriptors.
`crates/atlas-cli` (1 file)	Scriptable CLI subcommands: `presets` , `metrics` , `criticality` , `topology` , `path` , `lesion` , `export-json` , and `export-swc` .
`crates/atlas-gui` (3 files)	Interactive 3D viewport, matrix heatmap, lesion console, native `rfd` dialogs, `VERSIONINFO` icon embedding, and 1600 × 1000 offscreen PNG capture.

Figure 1. Offscreen Headless GPU Capture (1600 × 1000 RGBA): Human MNI152 Stereotaxic Inspector



Offscreen GPU capture displaying surgical octant cutaway of 3D gyral cerebral hemispheres exposing Corpus Callosum, Thalamus, Hippocampus, Brainstem, Cerebellum, 40 ROIs, 62 white-matter tracts, and triplanar 2D slices.

3. Cross-Species Structural, Criticality & Persistent Homology Benchmarks

Deterministic CLI execution across all four bundled species atlases demonstrates distinct evolutionary topological signatures while preserving critical dynamical amplification (Table 2; Figure 2). *Homo sapiens* (40 nodes, 62 edges) achieves the highest global routing efficiency (**0.26475**) across the longest characteristic path (**4.8583** steps, mean conduction delay **7.3635 ms**) and supports **14** persistent beta$_1$ topological loops (max persistence **0.85**). By contrast, compact *Drosophila melanogaster* FlyWire neuropils (22 nodes, 32 edges) concentrate integrative traffic into the strongest top-quartile rich club (**0.38095**) and widest stimulus dynamic range (**23.857 dB**), whereas *Caenorhabditis elegans* achieves peak mean clustering (**0.28883**) along its serial ventral-cord ganglia and *Mus musculus* Allen CCFv3 minimizes physical conduction delay (**2.9706 ms**).

Table 2. Cross-Species Structural Metrics, Branching Criticality & Z2 Persistent Homology

Preset	Species	N / E	Global Eff.	Path Len.	Clustering	Rich-Club	Dyn. Range	beta1 (Max P.)
`human_mni152`	*Homo sapiens*	40 / 62	0.26475	4.8583	0.2168	0.1304	22.697 dB	14 (0.85)
`mouse_ccfv3`	*Mus musculus (C57BL/6J)*	28 / 39	0.13434	3.8779	0.2269	0.3056	21.923 dB	3 (0.78)
`drosophila_flywire`	*Drosophila melanogaster*	22 / 32	0.13729	2.6032	0.1515	0.3810	23.857 dB	7 (0.85)
`celegans_wormatlas`	*Caenorhabditis elegans*	26 / 35	0.14996	3.3471	0.2888	0.2273	22.169 dB	4 (0.83)

Structural perturbation experiments on the Human MNI152 connectome isolate hierarchical vulnerability between midline association trunks and focal cortical hubs (Table 3). Severing the longitudinal `Cingulum Bundle` inflicts the sharpest network degradation, dropping global efficiency by 19.66% (**80.34%** retained: `0.26475 → 0.21269`) and disconnecting the graph into two components; severing the interhemispheric `Corpus Callosum` retains **87.82%** efficiency (2 components), while ablating the Posterior Cingulate hub `DMN.PCC` retains **88.31%** (2 components) versus **93.44%** for unilateral sensorimotor node `SMN.Lat_L` (remaining 1 connected component). Shortest weighted corticocerebellar tracing between `DMN.MPFC` and right cerebellum `CBL.Crus1_R` traverses 5 hops (`DMN.MPFC → SAL.ACC → SUBC.Thal_L → SMN.Lat_L → BSTEM.Pons → CBL.Crus1_R`) with **345.73 mm** geometric arc length, **36.01 ms** summed conduction latency, and bottleneck weight **0.76**.

Table 3. Simulated Structural Lesion Impact on Human MNI152 Global Efficiency

Target Perturbed	Intervention Class	Intact Eff.	Lesioned Eff.	Retained Eff.	Components
Corpus Callosum	White-Matter Tract	0.26475	0.23250	87.82%	1 → 2
Cingulum Bundle	White-Matter Tract	0.26475	0.21269	80.34%	1 → 2
`DMN.PCC`	Cortical Hub Node	0.26475	0.23379	88.31%	1 → 2
`SMN.Lat_L`	Cortical Hub Node	0.26475	0.24738	93.44%	1 → 1

Figure 2. Cross-Species Connectome Benchmarks & Human MNI152 Lesion Profile

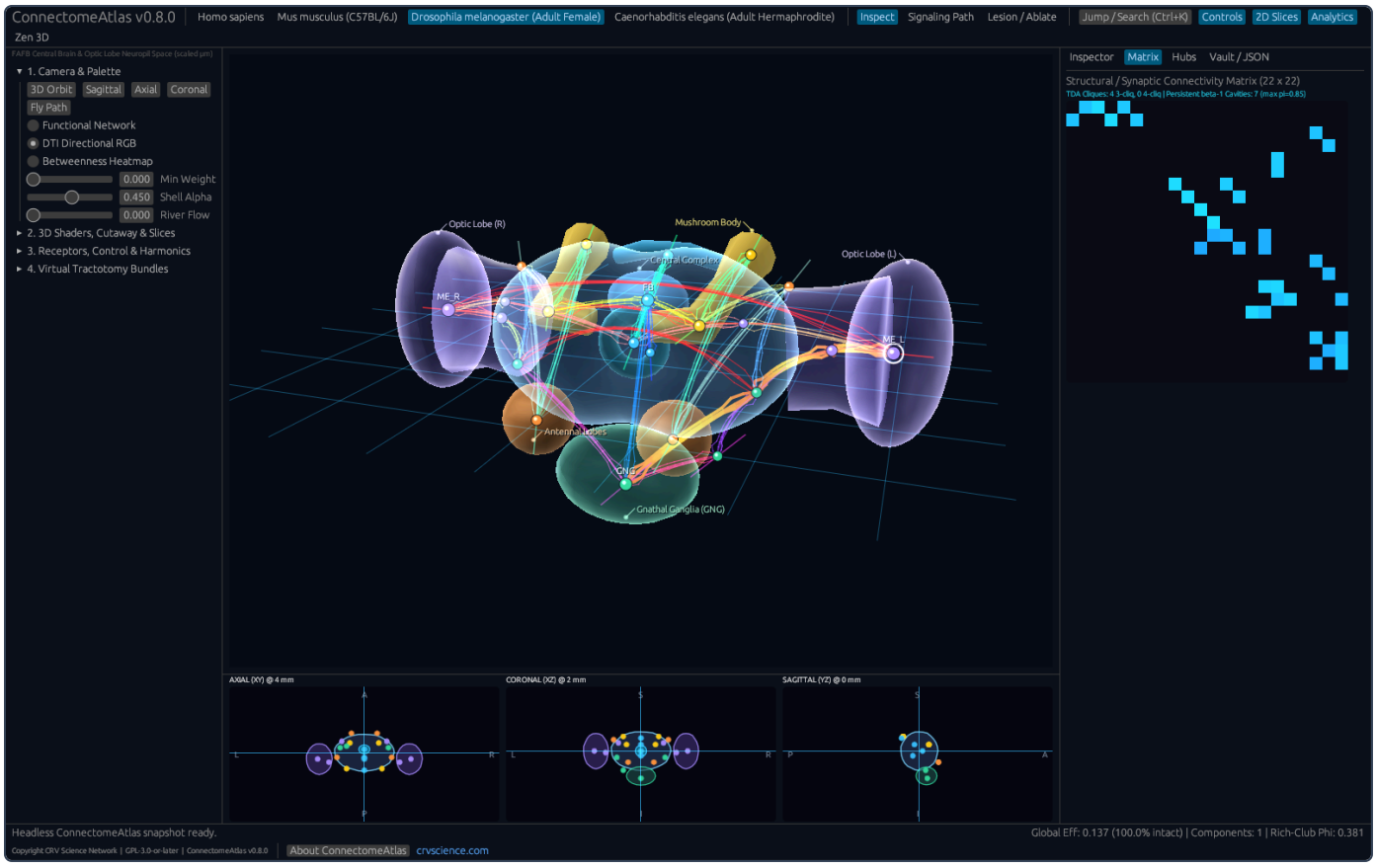


Left: Weighted global efficiency, stimulus dynamic range (dB), rich-club coefficient, and Z_2 persistent beta_1 loops across 4 species. Right: Human MNI152 lesion efficiency retention and five-crate workspace pipeline.

4. Interactive Atlas Views & Neuroinformatics I/O

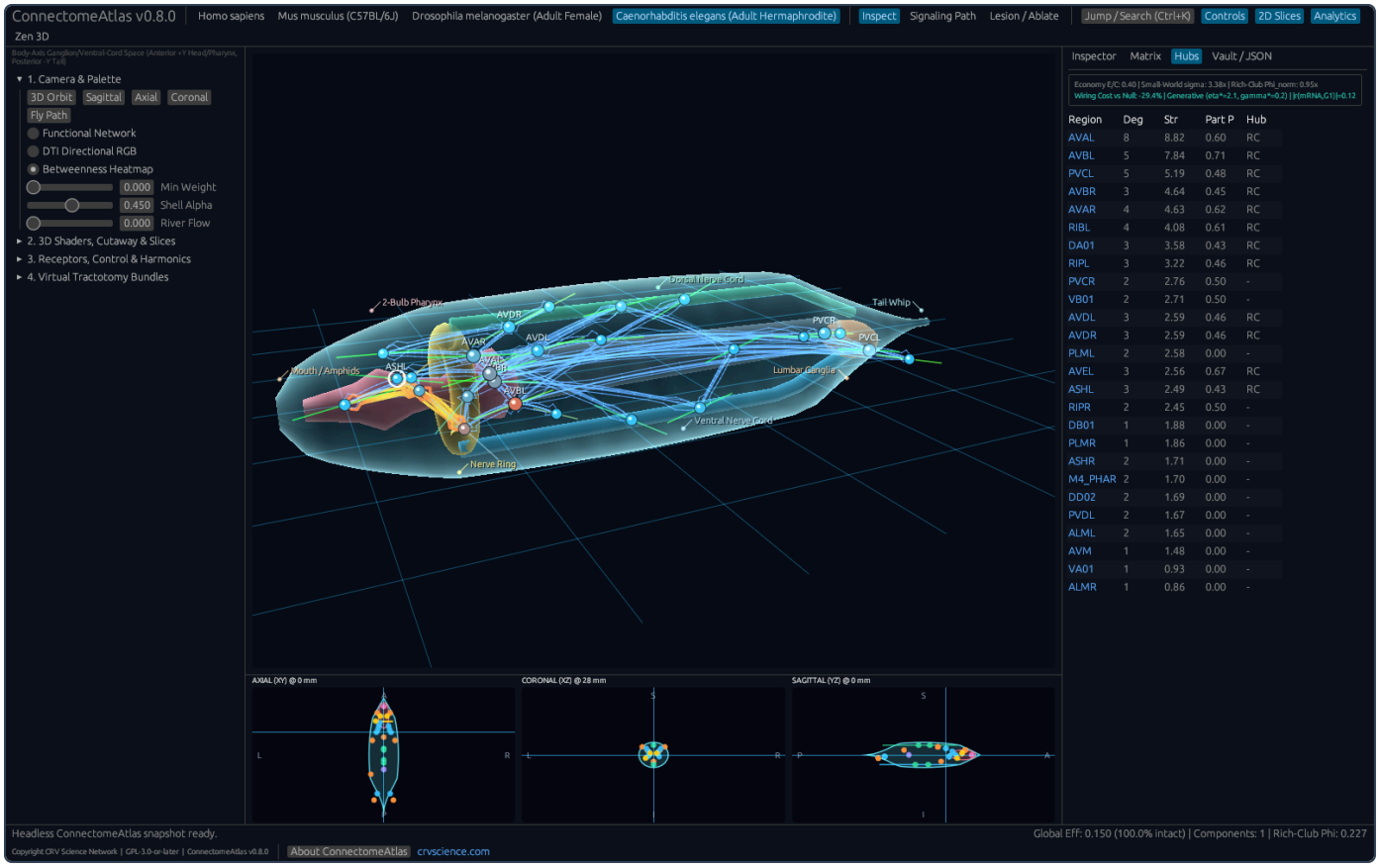
Beyond stereotaxic cortical streamlines, ConnectomeAtlas renders ordered adjacency connectivity matrices, receptor/transcriptomic node overlays, and inter-species 3D anatomy cleanly at native resolution (Figures 3–4). For interoperable data exchange, `atlas-io` parses compressed NIfTI-1 neuroimaging headers (`.nii.gz`), TrackVis streamline binary files (`.trk`), SQLite WAL persistence vaults, SWC neuronal arbor morphology reconstructions, and tamper-evident SHA-256 JSON worksets (`AtlasEnvelope`) validated across all 12 workspace unit and integration tests.

Figure 3. Headless Interface Gallery: Drosophila melanogaster FlyWire Neuropils & Matrix



Headless 1600 × 1000 capture displaying *Drosophila* FlyWire FAFB bilateral optic lobes, central complex (EB/FB/PB), antennal lobes, mushroom bodies, gnathal ganglia, connectivity matrix, and triplanar cross-sections.

Figure 4. Headless Interface Gallery: Caenorhabditis elegans Cuticle, Pharynx & Ganglion Hubs



Headless 1600 × 1000 capture showing *C. elegans* translucent annulated cuticle body, two-bulb pharynx, circumpharyngeal nerve ring, dorsal/ventral nerve cords, rich-club hub ranking, and triplanar slices.

5. Discussion

Comparing macroscopic tract atlases alongside compact invertebrate wiring diagrams highlights how persistent homology and criticality metrics complement standard graph summaries[2–4]. While Human MNI152 maximizes global efficiency (`0.26475`) via long-range association and callosal bridges that generate 14 redundant beta_1 cycles, losing either the Cingulum Bundle or the Corpus Callosum immediately splits graph connectivity and cuts global routing by 12–20%. Current bundled presets represent canonical parcellated circuits rather than voxel-wise whole-brain connectomes containing millions of edges; extending sparse GPU matrix eigensolvers and empirical diffusion tractography imports across larger HCP parcellations defines the next release roadmap.

6. Software Availability & Network Integration

ConnectomeAtlas (v0.8.0) is distributed as open-source Rust software under the GNU General Public License v3.0 or later (GPL-3.0-or-later) at https://crvscience.com/apps[6–25]. Within the twenty-application CRV Science suite, ConnectomeAtlas pairs directly with NeuroSpace Lab (microscale laminar cortical plasticity and optogenetic lesions), Causal-Atlas (transcriptomic pathway flips), Cit-Atlas (spectral graph modularity), and QuantaCrypt-Studio (linear-algebra and Hilbert-space eigenanalysis).

References

1. **[1]** Sporns, O., Tononi, G., & Kotter, R. (2005). The Human Connectome: A Structural Description of the Human Brain. PLOS Computational Biology, 1(4), e42. https://doi.org/10.1371/journal.pcbi.0010042
2. **[2]** Rubinov, M., & Sporns, O. (2010). Complex network measures of brain connectivity: Uses and interpretations. NeuroImage, 52(3), 1059–1069. https://doi.org/10.1016/j.neuroimage.2009.10.003
3. **[3]** Beggs, J. M., & Plenz, D. (2003). Neuronal Avalanches in Neocortical Circuits. The Journal of Neuroscience, 23(35), 11167–11177. https://doi.org/10.1523/JNEUROSCI.23-35-11167.2003

4. **[4]** Giusti, C., Ghrist, R., & Bassett, D. S. (2016). Two's company, three (or more) is a simplex. Journal of Computational Neuroscience, 41(1), 1–14. https://doi.org/10.1007/s10827-016-0608-6
5. **[5]** Dorkenwald, S., Matsliah, A., Yu, S. C., et al. (2024). Neuronal wiring diagram of an adult brain. Nature, 634, 124–138. https://doi.org/10.1038/s41586-024-07558-y
6. **[6]** White, B. P. (2026). The CRV Science App Network: Twenty Open-Source Rust Programs for Science, Data, and Simulation. CRV Science App Preprint APP-PREPRINT-01 [cs.SE, cs.CE, q-bio.QM], v1.1.0. Hosted via CRV Science Apps Hub (https://crvscience.com/apps). https://doi.org/10.5281/zenodo.24222398
7. **[7]** White, B. P. (2026). AeroFlyway: Tracking Bird Migration with Weather Radar, Skyglow Maps, and Nighttime Flight Calls. CRV Science App Preprint APP-PREPRINT-13 [q-bio.PE, physics.ao-ph, cs.GR], v0.6.0. Hosted via CRV Science Apps Hub (https://crvscience.com/apps). https://doi.org/10.5281/zenodo.24222366
8. **[8]** White, B. P. (2026). BeoFold: Simulating How Proteins Fold Using Distributed Computing and State Networks. CRV Science App Preprint APP-PREPRINT-02 [q-bio.BM, physics.chem-ph, cs.DC], v1.4.0. Hosted via CRV Science Apps Hub (https://crvscience.com/apps). https://doi.org/10.5281/zenodo.24222370
9. **[9]** White, B. P. (2026). Calc-Lab: Interactive Calculus, Linear Algebra, and Differential Equation Solver Workbench. CRV Science App Preprint APP-PREPRINT-03 [math.NA, cs.MS, cs.CY], v0.5.0. Hosted via CRV Science Apps Hub (https://crvscience.com/apps). https://doi.org/10.5281/zenodo.24222372
10. **[10]** White, B. P. (2026). Causal-Atlas: Tracing How Genes and Drugs Turn Biological Pathways On and Off. CRV Science App Preprint APP-PREPRINT-04 [q-bio.MN, q-bio.GN, stat.ML], v0.2.0. Hosted via CRV Science Apps Hub (https://crvscience.com/apps). https://doi.org/10.5281/zenodo.24222376
11. **[11]** White, B. P. (2026). Cit-Atlas: Mapping Citation Networks and Research Impact Across Scientific Papers. CRV Science App Preprint APP-PREPRINT-05 [cs.DL, cs.SI, physics.soc-ph], v1.8.0. Hosted via CRV Science Apps Hub (https://crvscience.com/apps). https://doi.org/10.5281/zenodo.24222380
12. **[12]** White, B. P. (2026). EpiLedger: Privacy-Safe Disease Tracking, Clinical Text Screening, and Outbreak Monitoring. CRV Science App Preprint APP-PREPRINT-06 [cs.CR, q-bio.PE, stat.AP], v2.0.0. Hosted via CRV Science Apps Hub (https://crvscience.com/apps). https://doi.org/10.5281/zenodo.24222382
13. **[13]** White, B. P. (2026). ITME: Modeling Evolutionary Regimes, Contingency, and Substrate Complexity Across Molecular, Hominid, and AI Worlds. CRV Science App Preprint APP-PREPRINT-07 [q-bio.PE, nlin.AO, physics.bio-ph], v2.3.0. Hosted via CRV Science Apps Hub (https://crvscience.com/apps). https://doi.org/10.5281/zenodo.24222386
14. **[14]** White, B. P. (2026). OSABT: A 20-Module Biology and Biostatistics Workbench for Molecular Labs, Genetics, Kinetics, and Ecology. CRV Science App Preprint APP-PREPRINT-08 [q-bio.QM, stat.AP, cs.SE], v2.0.0. Hosted via CRV Science Apps Hub (https://crvscience.com/apps). https://doi.org/10.5281/zenodo.24222388
15. **[15]** White, B. P. (2026). SAR-Atlas: Drug Design, Body Distribution Modeling, and Candidate Screening in Rust. CRV Science App Preprint APP-PREPRINT-09 [physics.chem-ph, q-bio.BM, cs.LG], v3.8.0. Hosted via CRV Science Apps Hub (https://crvscience.com/apps). https://doi.org/10.5281/zenodo.24222390
16. **[16]** White, B. P. (2026). TerraTwin: Fast Climate Projections for Global Warming, Sea-Level Rise, and Arctic Change. CRV Science App Preprint APP-PREPRINT-10 [physics.ao-ph, cs.CE, stat.AP], v2.5.0. Hosted via CRV Science Apps Hub (https://crvscience.com/apps). https://doi.org/10.5281/zenodo.24222392
17. **[17]** White, B. P. (2026). Urban-Grid: Modeling City Traffic, Emergency Response Coverage, and Earthquake Evacuation. CRV Science App Preprint APP-PREPRINT-11 [physics.soc-ph, cs.MA, cs.CE], v5.2.0. Hosted via CRV Science Apps Hub (https://crvscience.com/apps). https://doi.org/10.5281/zenodo.24222394
18. **[18]** White, B. P. (2026). WildFront BattleGrounds: Turn-Based Hex Strategy Game with Voxel Graphics and Procedural Map Generation. CRV Science App Preprint APP-PREPRINT-12 [cs.GT, cs.GR, math.CO], v3.4.1. Hosted via CRV Science Apps Hub (https://crvscience.com/apps). https://doi.org/10.5281/zenodo.24222396
19. **[19]** White, B. P. (2026). HelioProbe: Simulating Spacecraft Orbits, Deep-Space Telescopes, and Comet Tails in 3D. CRV Science App Preprint APP-PREPRINT-14 [astro-ph.EP, astro-ph.IM, cs.GR], v2.3.0. Hosted via CRV Science Apps Hub (https://crvscience.com/apps). https://doi.org/10.5281/zenodo.24244083
20. **[20]** White, B. P. (2026). PopBio-Studio: Interactive Population Biology, Adaptive Landscapes, and Genetic Skyline Simulator. CRV Science App Preprint APP-PREPRINT-15 [q-bio.PE, q-bio.QM, stat.AP], v1.2.0. Hosted via CRV Science Apps Hub (https://crvscience.com/apps). https://doi.org/10.5281/zenodo.24244085

21. **[21]** White, B. P. (2026). QuantaCrypt-Studio: Simulating Quantum Circuits, Quantum Key Distribution, and Post-Quantum Cryptography. CRV Science App Preprint APP-PREPRINT-16 [quant-ph, cs.CR, cs.MS], v2.2.0. Hosted via CRV Science Apps Hub (https://crvscience.com/apps). https://doi.org/10.5281/zenodo.24244089

22. **[22]** White, B. P. (2026). SonoWing: Analyzing Bat Echolocation and Bird Calls with Spectrograms and Harmonic Tracking. CRV Science App Preprint APP-PREPRINT-17 [q-bio.NC, q-bio.PE, cs.SD], v1.1.0. Hosted via CRV Science Apps Hub (https://crvscience.com/apps). https://doi.org/10.5281/zenodo.24244091

23. **[23]** White, B. P. (2026). SwarmForge: 3D Isometric Automated Factory and Swarm Robotics Simulation Game. CRV Science App Preprint APP-PREPRINT-18 [cs.MA, cs.RO, cs.GT], v1.3.0. Hosted via CRV Science Apps Hub (https://crvscience.com/apps). https://doi.org/10.5281/zenodo.24244093

24. **[24]** White, B. P. (2026). NeuroSpace Lab: 3D Neural Network Topology, Structural Plasticity, and Six-Layered Cerebral Cortex Simulation in Rust. CRV Science App Preprint APP-PREPRINT-19 [q-bio.NC, cs.NE, cs.GR], v1.6.0. Hosted via CRV Science Apps Hub (https://crvscience.com/apps). https://doi.org/10.5281/zenodo.24263468

25. **[25]** White, B. P. (2026). TrophicHearth: Nine-Biome 3D Living Trophic Diorama, Fire-Pit Hearth, and Bioacoustic Ecosystem Simulator in Rust. CRV Science App Preprint APP-PREPRINT-20 [q-bio.PE, cs.GR, cs.MA], v0.9.3. Hosted via CRV Science Apps Hub (https://crvscience.com/apps). https://doi.org/10.5281/zenodo.24359107